DOI: https://doi.org/10.17816/morph.627332

Changes in the pathomorphological condition of the myocardium in dysferlinopathy mice (Bla/J type)

Maria A. Savelyeva[1], Sergey N. Bardakov[2], Alexey M. Emelin[1], Roman V. Deev[3]

[1] North-Western State Medical University named after I.I. Mechnikov, Saint Petersburg, Russia;
[2] S.M. Kirov Military Medical Academy, Saint Petersburg, Russia;
[3] Russian Research Center of Surgery named after Academician B.V. Petrovsky, Moscow, Russia

ABSTRACT

BACKGROUND: Dysferlinopathy is heritable progressive muscular dystrophy caused by *DYSF* mutation. Currently, although skeletal muscle pathology has been defined, only fragmentary and limited myocardium histopathology data are available.

AIM: The study aimed to analyze the pathomorphological status of the myocardium in Bla/J mice models of dysferlinopathy at different ages.

MATERIALS AND METHODS: Data from two experimental groups were analyzed: Bla/J mice with *DYSF* knockout on 3, 6, and 12 months old and control wild-type Balb/C mice aged 6 months. The expressions and patterns of dyeing of protein dysferlin in the immunofluorescent search method were analyzed. These were held such parameters of the histological characteristic of the myocardium of three dyeing protocols (hematoxylin and eosin, iron hematoxylin by Rego, and hematoxylin-basic fuchsin-picric acid by Lie), and morphometry of the parameters of the cardiomyocytes (length, width of cardiomyocytes, and nuclear perimeter).

RESULTS: The immunofluorescent search method revealed high levels of dysferlin in the myocardium of the control group. Statistical analysis showed significant differences between Bla/J and Balb/C mice: the increasing length and width of cardiomyocytes in dysferlinopathy by 49.9% ((95% confidence interval, 45.9–57.4) and 35.6 (95% confidence interval, 32.9–37.9)), respectively. Nucleus perimeter was significantly reduced in the dysferlinopathy group with disease duration of 6 months (by 23.9 (95% confidence interval, 20.2–27.5) compared with the group with disease duration of 3 months and by 18.8% (95% confidence interval, 8.5–19.7)) and the control group. Consequently, progressive hypertrophy of cardiomyocytes, increasing deformation in cardiomyocytes, intercalated disk destruction, hypoxia features, and necrosis indication were observed, resulting in fibrosis. A pattern of cardiomyocyte size reduction dependent on the aging process was observed.

CONCLUSIONS: Dysferlin deficiency leads to significant damage in the myocardium of Bla/J mice.

Keywords: heart; myocardium; Bla/J mice; dysferlinopathy.

To cite this article:
Savelyeva MA, Bardakov SN, Emelin AM, Deev RV. Changes in the pathomorphological condition of the myocardium in dysferlinopathy mice (Bla/J type). *Morphology*. 2023;161(3):9–18. DOI: https://doi.org/10.17816/morph.627332

Received: 04.03.2024 **Accepted:** 09.04.2024 **Published:** 15.04.2024

DOI: https://doi.org/10.17816/morph.627332

Патоморфологическая характеристика миокарда мышей с дисферлинопатией (линия Bla/J)

М.А. Савельева[1], С.Н. Бардаков[2], А.М. Емелин[1], Р.В. Деев[3]

[1] Северо-Западный государственный медицинский университет имени И.И. Мечникова, Санкт-Петербург, Россия;
[2] Военно-медицинская академия имени С.М. Кирова, Санкт-Петербург, Россия;
[3] Российский научный центр хирургии имени академика Б.В. Петровского, Москва, Россия

АННОТАЦИЯ

Обоснование. Дисферлинопатия — наследственная прогрессирующая мышечная дистрофия, причиной развития которой являются мутации в гене *DYSF*. Патоморфологические изменения поперечнополосатой скелетной мускулатуры детально описаны при снижении экспрессии дисферлина или при его полном отсутствии, в то время как данные о гистопатологии миокарда при дисферлинопатии фрагментарны и ограничены.

Цель исследования — оценить структурные изменения миокарда в разные возрастные периоды у мышей линии Bla/J, являющейся моделью дисферлинопатии.

Материалы и методы. Исследовали нокаутную по гену *DYSF* линию мышей Bla/J на сроках 3, 6 и 12 мес с момента рождения. Контрольную группу составили мыши линии Balb/C в возрасте 6 мес. Проводили иммунофлуоресцентную детекцию белка дисферлина в миокарде с оценкой его наличия и распределения в кардиомиоцитах. Анализировали структуру миокарда в парафиновых срезах с применением окраски гематоксилином и эозином, железным гематоксилином по Рего и ГОФПК по Ли. Провели морфометрию длины, толщины кардиомиоцитов и измерили периметр их ядер у мышей линии Bla/J.

Результаты. Дисферлин был выявлен только в миокарде мышей контрольной группы. При 95% доверительном интервале (ДИ) длина кардиомиоцитов мышей с нокаутом гена *DYSF* во всех возрастах была статистически значимо больше, чем у животных контрольной группы, максимально на 49,9 (45,9–57,4)%; толщина кардиомиоцитов — на 35,6 (32,9–37,9)%; периметр ядер кардиомиоцитов мышей линии Bla/J в возрасте 6 мес был меньше на 23,9 (20,2–27,5)%, чем у мышей линии Bla/J трёхмесячного возраста, и на 18,8 (8,5–19,7)% меньше по сравнению с контролем. У мутантных мышей выявлены прогрессирующая по сравнению с нормой гипертрофия кардиомиоцитов, нарастающая деформация кардиомиоцитов, разрушение их вставочных дисков, признаки гипоксии и некроза с исходом в фиброз. С увеличением возраста животных размер клеток миокарда уменьшался.

Заключение. Дефицит белка дисферлина приводит к значимым структурным изменениям миокарда у мышей линии Bla/J.

Ключевые слова: сердце; миокард; мыши линии Bla/J; дисферлинопатия.

Как цитировать:
Савельева М.А., Бардаков С.Н., Емелин А.М., Деев Р.В. Патоморфологическая характеристика миокарда мышей с дисферлинопатией (линия Bla/J) // Морфология. 2023. Т. 161, № 3. С. 10–18. DOI: https://doi.org/10.17816/morph.627332

Рукопись получена: 04.03.2024 **Рукопись одобрена:** 09.04.2024 **Опубликована:** 15.04.2024

BACKGROUND

Dysferlinopathy is a hereditary progressive muscular dystrophy characterized by distal, proximal, proximodistal, and congenital variants of clinical phenotypes [1]. Its worldwide prevalence is 1 per 200,000 newborns [2, 3]. Inheritance is predominantly autosomal recessive; however, a dominant type has also been described [4, 5]. Dysferlinopathy is caused by mutations in DYSF, which are localized to the short arm of the second chromosome [4]. Dysferlin ensures the repair of the sarcolemma and endoplasmic reticulum of muscle fibers of striated skeletal muscles. However, the significance of this protein in the cyto- and histophysiology of cardiomyocytes has not been sufficiently studied.

In 1999, L.V. Anderson et al. [7] established that dysferlin is expressed starting from weeks 5–6 of embryogenesis, is detected in many tissues, and mainly affects the development of muscle tissue [6, 7]. In dysferlin deficiency, the most pronounced pathological changes occur in the striated skeletal muscles. Extensive information has been accumulated on the pathomorphological signs of dystrophy in skeletal muscles of animals and humans [8–11]. In muscle fibers, ruptures and invaginations of the sarcolemma, subsarcolemmal accumulations of vesicles, vacuolization, mitochondrial fusion, expansion of the sarcoplasmic reticulum cisterns, and disorganization of myofibrils and T-tubules occur [8, 12]. These changes are caused by inefficient intracellular regeneration, resulting in necrosis, inflammation, lipoidosis, and fibrosis of the muscle fibers [8, 13]. Over the past 20 years, studies have highlighted the importance of dysferlin in myocardial function [14–17]. The dystrophic process in skeletal muscles is predominantly studied because of its priority involvement and greater accessibility to histological examination. Data on myocardial histopathology in dysferlinopathy are scattered and limited because cardiomyopathy does not have obvious clinical manifestations until the advanced stage of the disease and myocardial biopsy is impractical.

This study aimed to evaluate the pathological morphological changes in striated cardiac muscles in Bla/J mice with dysferlinopathy at different age periods.

MATERIALS AND METHODS

Study design

In this observational, single-center, prospective, full-design, controlled, non-randomized study, the myocardium of DYSF-mutant mice was chosen, and the pathomorphological changes in the myocardium of Bla/J mice were examined. The study aimed to determine and compare the myocardial structure of Bla/J mice with dysferlinopathy and Balb/C mice without dysferlinopathy. This study included qualitative (presence/absence of structural and metabolic changes) and quantitative assessments of cardiomyocytes (length, thickness, and nuclei perimeter of cardiomyocytes) on paraffin sections of the myocardium of animals in the study and control groups, followed by staining and morphometry. Paraffin sections were prepared according to a classical method [18]. Using the immunofluorescence method, the myocardium of the left ventricle of both groups was examined for the presence of dysferlin protein. For this purpose, heart muscle fragments were placed in isopentane and cooled in liquid nitrogen. The thickness of the cryosections was 10 μm. The animals were sacrificed by decapitation.

Objects (participants) of the study

This study included mice of the Bla/J line, which represents a model of dysferlinopathy (the line was created by inserting a retrotransposon into intron 4), and wild-type mice of the Balb/C line. The animals were 3–12 months old (inclusive).

Conditions

This study was conducted at the Department of Pathological Anatomy of the I.I. Mechnikov North Western State Medical University (St. Petersburg).

Main research outcome

The study endpoint was the description of the pathological characteristics of the myocardium in dysferlinopathy mice and their comparison with those of healthy mice.

Analysis in subgroups

The study group included seven male Bla/J mice aged 3, 6, and 12 months (n = 3, 3, and 1, respectively) as a model of dysferlinopathy. The control group included two healthy male Balb/C mice aged 6 months. Comparisons were made within each group and between each age subgroup of the Bla/J and Balb/C lines.

Methods of outcome registration

Paraffin sections of the myocardium were stained with hematoxylin and eosin and iron hematoxylin according to Rego to assess the preservation of the striated muscle tissue of the myocardium [19], and hematoxylin–basic fuchsin–picric acid (HBFPA) according to Lee to identify signs of hypoxic damage to cardiomyocytes [19].

The cardiomyocytes were characterized by morphometric accounting of three parameters, namely, the distance between the intercalated discs (length), thickness, and perimeter of the nuclei (2D format in the AxioVision v. 4.9.1 program, USA).

Cryosections were performed using primary rabbit monoclonal antibodies against dysferlin (ab124684, 1:200; Abcam, UK). Alexa Fluor 647 was used as a secondary antibody at a dilution of 1:200 (Invitrogen, USA), with nuclear staining with DAPI (Servicebio, China). The preparations were scanned using a Pannoramic 250 Flash microscope (3DHISTECH, Hungary).

Ethical considerations

The animal experiments were approved by the local ethical committee of the Kazan (Volga Region) Federal University (Protocol No. 14 of 02/08/2019). The maintenance of mice and all manipulations were performed in accordance with the principles of the European Convention for the Protection of Vertebrate Animals Used for Experimental and Other Scientific Purposes (Strasbourg, 2006).

Statistical analysis

The sample size was not precalculated. To analyze the results, descriptive and analytical statistical tools were used, implemented in Past v. 4.09 (Norway) [20]. To check the statistical homogeneity of several samples, one-factor (Friedman test) and two-factor (Kruskal–Wallis test) analyses of variance were used. The central tendencies of the samples were presented as means (M) and medians (Me), depending on compliance/non-compliance with the normal distribution. The variance of central tendencies was presented as 95% confidence intervals (CIs), calculated using bootstrap and Monte Carlo methods. For the subsequent identification of heterogeneous groups, multiple comparison procedures were used, namely the Mann–Whitney test with Bonferroni correction, and the Spearman rank correlation coefficient was applied for the correlation analysis. The linear dependence of the variables was described using the equation of paired linear regression ($y=bx+a$), where b (slope) is the angular coefficient and a (intercept) is the free member of the assessment line, for which 95% CIs were also calculated. Statistical hypotheses were tested using p values and 95% CI, whereas absolute and relative effect sizes were assessed for the differences studied [21, 22]. The relative effect sizes were calculated using Cohen's *dC* method (Cohen). CIs for *dC* were calculated using the EffectSizeCalculator.xls spreadsheet and the Effect Size Generator.xls program. For the graphical implementation of the data, the interactive program BoxPlotR (http://shiny.chemgrid.org/boxplotr/) was used.

RESULTS

Main research results

At the age of 3 months, the cardiomyocytes of Bla/J mice had a parallel orientation, were not deformed, and had no signs of discomplexation. At the age of 6 months, the arrangement of cardiomyocytes was not parallel, and at the age of 12 months, signs of loss of tissue complexity and wave-like deformity of muscle cells were observed, whereas the thickness (diameter) of cardiomyocytes increased (Fig. 1).

The morphometric characteristics of cardiomyocytes from the Bla/J and control groups differed significantly with respect to several parameters (Fig. 2). The length of cardiomyocytes in Bla/J mice at all stages was statistically significant greater than that in the control group, with a maximum at the age of 3 months (49.9% (95% CI, 45.9–57.4), $p=5.4\times10^{-48}$, Table 1). Moreover, the Bla/J line subgroups differed significantly from each other, with a trend toward a decrease in the length of cardiomyocytes with increasing age. This phenomenon is described by the linear regression equation: $y=-6.51x+254.33$ (95% CI, slope –8.7; –4.2; intercept, 240.8; 267.9; $p=1.5\times10^{-6}$). Thus, the age of the animals and length of the cardiomyocytes demonstrated a linear relationship.

The thickness (diameter) of the cardiomyocytes of Bla/J line mice of all age subgroups was statistically significantly greater than that in the control group, with a maximum value at the age of 6 months (35.6% (95% CI, 32.9–37.9) $p=8.4\times10^{-59}$). No statistically significant differences in this parameter were found between the ages of the Bla/J line animals.

When assessing the perimeter of the nuclei of cardiomyocytes, which is an indirect sign of synthetic cell activity, this parameter significantly decreased in the 6-month-old Bla/J subgroup by 23.9% (95% CI, 20.2–27.5) compared with the 3-month-old Bla/J subgroup ($p=0.04$) and by 18.8% (95% CI, 8.5–19.7) compared with the control group ($p=8.4\times10^{-59}$). The decrease in the perimeter of the nuclei with increasing monitoring time in the experimental group was described by the linear regression equation $y=-0.63x+101$ (95% CI, slope –1.1; –0.2; intercept 98.4; 104.6; $p=0.008$). The nuclear perimeter and duration of observation in the experimental group demonstrated a linear relationship.

Staining with iron hematoxylin in Bla/J mice aged ⩾3 months revealed diffuse intermuscular fibrosis of the myocardium, disappearance of cross-striations in some cardiomyocytes, and destruction of intercalated discs (Fig. 3*a*). In the control group (Balb/C), the myocardium was intact, with parallel orientation of the cardiomyocytes,

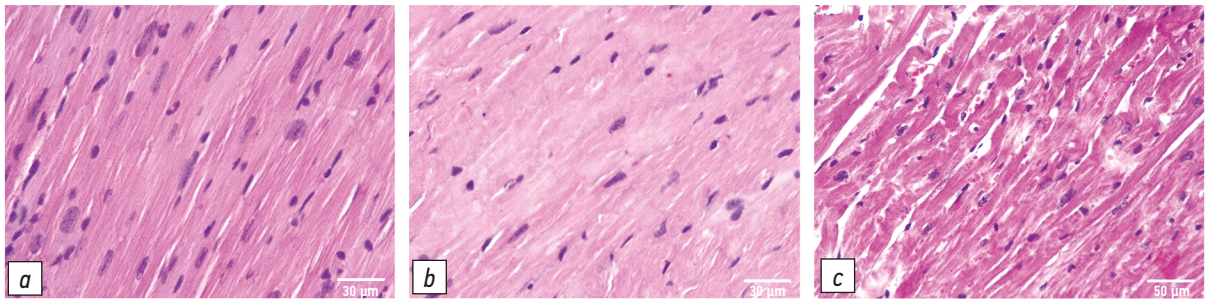

Fig. 1. Axial section of myocardium in Bla/J mice 3 (*a*), 6 (*b*), 12 (*c*) months old. Hematoxylin and eosin dying; ×200.
Рис. 1. Продольные срезы миокарда мышей линии Bla/J в возрасте 3 (*a*), 6 (*b*), 12 (*c*) мес. Окраска гематоксилином и эозином; ×200.

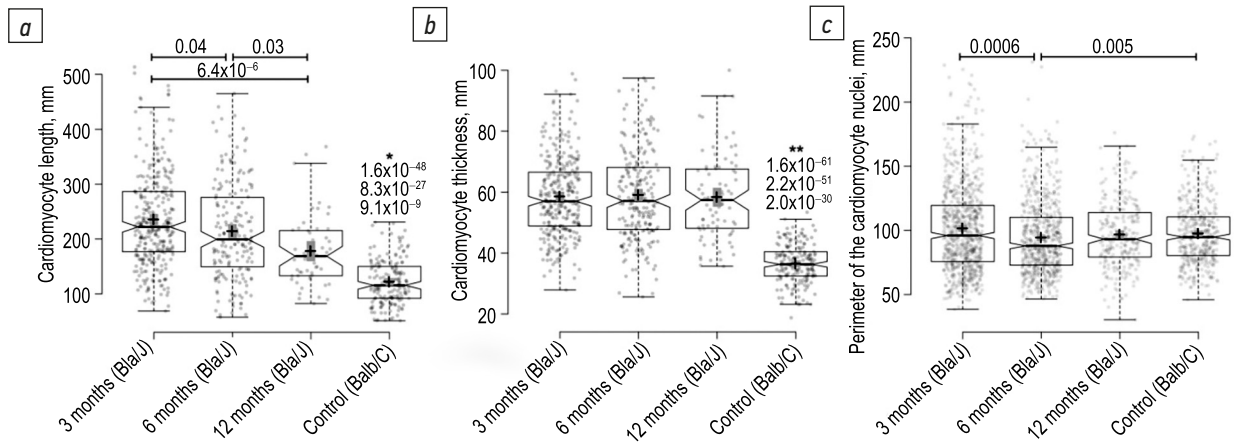

Fig. 2. Morphometric characteristics of cardiomyocytes in Bla/J and Balb/C mice: *a* — cardiomyocytes length; *b* — cardiomyocytes width (diameter); *c* — cardiomyocytes nucleus perimeter; * *p*-value in «cardiomyocytes length» comparison of every group of Bla/J mice with Balb/C mice, ** *p*-value in «cardiomyocytes width (diameter)» comparison of every group of Bla/J mice with Balb/C mice.
Рис. 2. Морфометрические характеристики кардиомиоцитов мышей линии Bla/J и Balb/C: *a* — длина кардиомиоцитов; *b* — толщина (диаметр) кардиомиоцитов; *c* — периметр ядер кардиомиоцитов; * значение *p* при сравнении каждой из групп Bla/J с Balb/C по характеристике «длина кардиомиоцитов», ** значение *p* при сравнении каждой из групп Bla/J с Balb/C по характеристике «толщина кардиомиоцитов».

Table 1. Differences in morphometric parameters of cardiomyocytes of compared Bla/J and Balb/C mice groups in different age
Таблица 1. Различия морфометрических параметров кардиомиоцитов мышей линий Bla/J и Balb/C разных возрастов

Comparison groups	Absolute effect size. μm (95% CI)	Relative effect size. % (95% CI)	Cohen's effect size	*p*
Cardiomyocyte length				
Bla/J 3 months and Bla/J 6 months	21.39 (5.7–37.1)	12.8 (6.9–19.5)	–0.24	0.007
Bla/J 6 months and Bla/J 12 months	36.11(10.6–61.6)	37.9 (33.9–49.2)	–0.42	0.005
Bla/J 3 months and Balb/C	113.7 (127.4–99.9)	49.9 (45.9–57.4)	–1.50	5.4×10^{-48}
Bla/J 6 months and Balb/C	92.3 (78.1–106.6)	42.9 (37.4–51.1)	–1.30	8.7×10^{-31}
Bla/J 12 months and Balb/C	56.2 (41.7–70.7)	34.6 (28.6–44.7)	–1.19	7.0×10^{-13}
Cardiomyocyte thickness				
Bla/J 3 months and Balb/C	22.1 (24.1–20.0)	34.0 (30.3–36.9)	–1.9	1.3×10^{-71}
Bla/J 6 months and Balb/C	22.6 (24.8–20.2)	35.6 (32.9–37.9)	–1.9	8.4×10^{-59}
Bla/J 12 months and Balb/C	21.9 (24.3–19.4)	33.4 (29.8–37.1)	–2.3	6.6×10^{-47}
Cardiomyocyte nucle				
Bla/J 3 months and Bla/J 6 months	7.1 (0.1–6.4)	23.9 (20.2–27.5)	–0.11	0.04
Bla/J 6 months and Balb/C	3.1 (24.8–20.2)	18.8 (8.5–19.7)	–1.9	8.4×10^{-59}

Note: according to the Cohen verbal scale (absolute) *dC* values from 0.2 to 0.5 are interpreted as a "weak" effect. from 0.5 to 0.8 — as a "moderate" effect and *dC* values ⩾0.8 as a "strong" effect.
Примечание: согласно вербальной шкале Коэна (абсолютные) значения *dC* от 0,2 до 0,5 трактуются как «слабый» эффект, от 0,5 до 0,8 — как «умеренный» эффект и значения *dC* ⩾0,8 — как «сильный» эффект.

preserved transverse striations, intercalated discs, and without fibrosis (Fig. 3*c*).

Lee staining with HBFPA in 3-month-old Bla/J mice revealed hypoxic changes such as diffuse fuchsinophile staining of cardiomyocytes (Fig. 3*b*). In the control group (Balb/C), no signs of hypoxic damage were observed in the myocardium (Fig. 3*d*).

During an immunofluorescent reaction test with antibodies to dysferlin in the myocardium of Bla/J mice at 3, 6, and 12 months of age, the protein was not detected (Fig. 4*a* presents the results of a study on the myocardium of animals at the age of 3 months). In the control group, the result was positive (Fig. 4*b*); dysferlin was presented as inclusions in the sarcoplasm and area of intercalated discs.

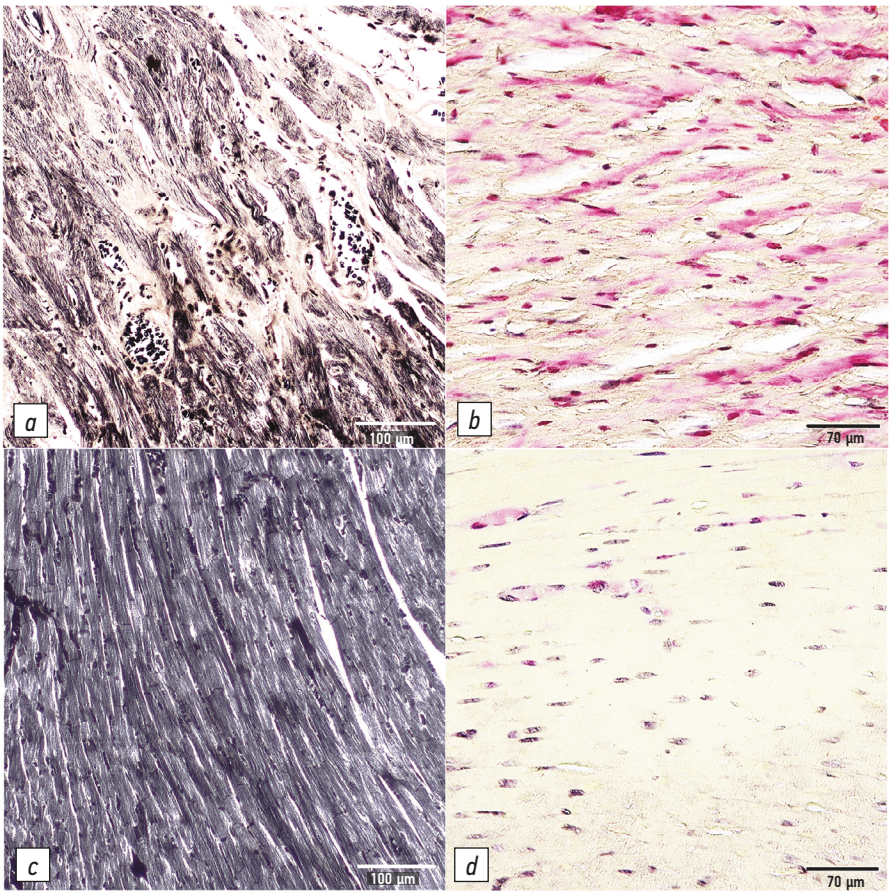

Fig. 3. Myocardium of Bla/J (*a*, *b*) and Balb/C (*c*, *d*) mice: *a* — 12 months old, intermuscular fibrosis; *b* — 6 months old, multiple fuchsinophilic insertions in cytoplasm; *c* — 6 months old, no fibrosis features; *d* — 6 months old, no fuchsinophilic insertions in cytoplasm. Iron hematoxylin dying (*a*, *c*); hematoxylin-basic fuchsin-picric acid dying (*b*, *d*); *a*, *c* — ×200; *b*, *d* — ×400.
Рис. 3. Миокард мышей линии Bla/J (*a*, *b*) и Balb/C (*c*, *d*): *a* — 12 мес, межмышечный фиброз; *b* — 6 мес, множественные фуксинофильные включения в цитоплазме; *c* — 6 мес, отсутствие признаков фиброза; *d* — 6 мес, отсутствие фуксинофильных включений в кардиомиоцитах. Окраска железным гематоксилином по Рего (*a*, *c*); окраска ГОФПК по Ли (*b*, *d*); *a*, *c* — ×200; *b*, *d* — ×400.

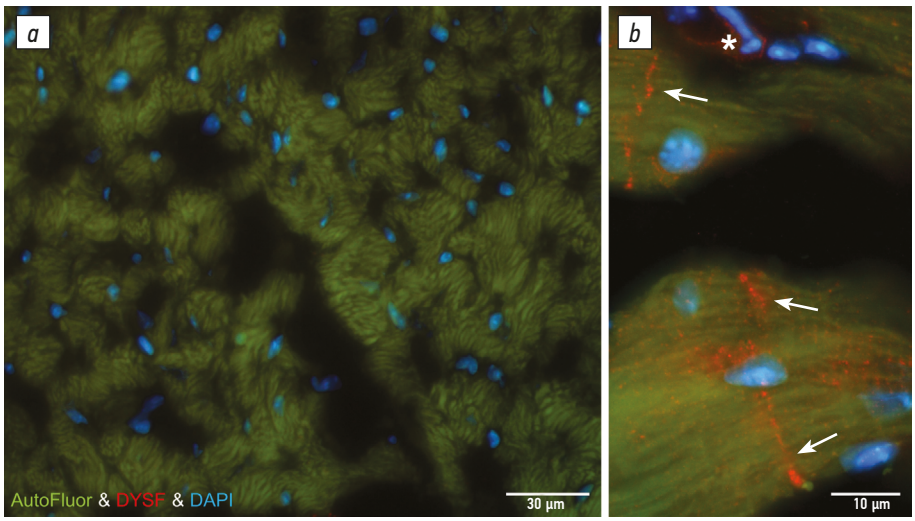

Fig. 4. Immunofluorescent reaction with dysferlin antynody: *a* — cross section of Bla/J mice cardiomyocytes; *b* — axial section Balb/C mice, the product of the reaction has perinuclear localisation and intercalated disks sites (→) and in endothelium (*). Green spectrum fluorescence is auto fluorescence of the cytoskeleton, red spectrum fluorescence is fluorescence of the detection system, blue spectrum fluorescence is nuclear coloring with DAPI; *a* — ×400; *b* — ×1000.
Рис. 4. Иммунофлуоресцентная реакция с антителами к дисферлину: *a* — поперечное сечение кардиомиоцитов мышей линии Bla/J; *b* — продольное сечение кардиомиоцитов мышей линии Balb/C, продукт реакции локализован перинуклеарно в области вставочных дисков (→) и в эндотелиоцитах (*). Свечение в зелёном спектре — аутофлуоресценция белков цитоскелета, свечение в красном спектре — свечение системы детекции, свечение в синем спектре — докраска ядер DAPI; *a* — ×400; *b* — ×1000.

DISCUSSION

Summary of main research result

In the myocardium of Bla/J mice, signs of tissue disruption were detected, with a tendency for the pathological changes to increase from 3 to 12 months. In the control group (with dysferlin), no such changes were revealed; therefore, the absence of dysferlin was the main factor in the development of pathomorphological changes in the myocardium.

Discussion of the main research result

In Bla/J line mice, the myocardium was characterized by a wave-like deformity of cardiomyocytes, disruption of the parallel orientation of cardiomyocytes, and hypoxic damage, which were not previously detected in the myocardium of animals of other artificial mouse lines with dysferlinopathy (A/J, C57BL/6J, and SJL/J lines) [23]. In addition, the disappearance of intercalated discs in animals with dysferlinopathy and a significant increase in the distance between intercalated discs were observed compared with animals in the control group. Similar changes, characterized by the destruction of up to one-third of the intercalated discs of cardiomyocytes, were previously revealed in the myocardium of C57BL/6J mice at the late stages of dysferlinopathy [24].

Significant thickening of cardiomyocytes was detected in all age groups of the Bla/J mice. Cardiomyocyte hypertrophy was probably caused by the remodeling of the cardiomyocyte T-system in the form of shortening of T-tubules and their axial reorientation and separation from sarcomeres [15, 25]. This pathological process causes a change in calcium homeostasis in cardiomyocytes, which determines the functioning of the calcium–calmodulin signaling pathway [26, 27]. Myocardial hypertrophy was also observed in dysferlin-deficient mice of the B6.129-*Dysf*^{tm1Kcam}/J line at the age of 3 months, with a significant increase in the ratio of myocardial mass to body weight in contrast to the control group (the differences in the body weights of both groups were not significant). In addition to the organ level, hypertrophic changes were observed in isolated cardiomyocytes of 3-month-old dysferlin-deficient mice in contrast to the control group [28]. Therefore, as dysferlinopathy progresses in mice, cardiomyocyte hypertrophy develops with age.

Intermuscular fibrosis in Bla/J mice was detected at the age of 3 months, in contrast to dysferlin-deficient B6.129-*Dysf*^{tm1Kcam}/J mice, in which fibrosis was detected only in the 20th month of life and was manifested by a threefold increase in the collagen level in the stroma compared to the control [15, 28]. A/J mice also did not show significant fibrosis [14]. Specifically, the proportion of collagen increased from 2% to 3% from month 2 to 18 of observation, and did not differ from the control group of A/HeJ mice [14]. Further studies on the variability in the severity of myocardial fibrosis among different strains of dysferlin-deficient mice are required.

Dysferlin in the myocardium of the control group of Balb/C mice was located at the perimeter of the nuclei, area of intercalated discs, and endothelial cells, which corresponds to previous information [12, 14, 15, 25]. Several researchers have also reported the presence of dysferlin in the tubular system of cardiomyocytes and near L-type calcium channels and ryanodine receptors [12, 25]. Dysferlin was not detected in the myocardium of Bla/J mice, which was presumed to be the cause of a cascade of pathological changes in the myocardium.

The results of the cardiac pathology studies in patients with limb-girdle muscular dystrophy R2 showed some parallel results in the present study. In particular, cases of dilated cardiomyopathy have been described, characterized by hypertrophy of cardiomyocytes in combination with an increase in nuclear size, interstitial fibrosis, or only variability in the size of cardiomyocytes and disorganization of their location [29, 30]. However, diffuse fibrosis and fatty infiltration of the myocardium can be detected in patients with dysferlinopathy even without clinical and instrumental signs of cardiomyopathy [16]. Thus, structural abnormalities may be noted in the myocardium of patients with dysferlinopathy, which were accompanied by functional changes in some cases [30].

Study limitations. Only one model of dysferlinopathy was evaluated, i.e., the Bla/J line, which complicates the extrapolation of the results to other models. In addition, the sample size required to achieve the required statistical power for the results was not calculated. In this regard, the sample collected was not representative, which does not allow extrapolation of the results and their interpretation to the general population.

CONCLUSIONS

Myocardial structural impairment in dysferlin-deficient Bla/J mice increases with age and is accompanied by cardiomyocyte hypertrophy and myocardial fibrosis. Dysferlin deficiency is a key factor in the pathomorphogenesis of cardiomyopathies in experimental animals, particularly the Bla/J line. The involvement of the myocardium in the pathological process of dysferlinopathy was confirmed by the detection of cardiomyocyte hypertrophy in dysferlin-deficient strains of mice and patients with limb-girdle muscular dystrophy R2. The variability in the severity of fibrotic changes in the myocardium of dysferlin-deficient mice and patients casts doubt on the obligatory nature of this morphological feature. These results expand our understanding of the mechanisms underlying the development of cardiomyopathy in dysferlinopathy.

ADDITIONAL INFORMATION

Funding source. The study was carried out with the financial support of the Ministry of Science and Higher Education of Russia, agreement No. 075-15-2021-1346.

Competing interests. The authors declare that they have no competing interests.

Authors' contribution. All authors made a substantial contribution to the conception of the work, acquisition, analysis, interpretation of data for the work, drafting and revising the work, final approval of the version to be published and agree to be accountable for all aspects of the work. M.A. Savelyeva — production of histological preparations, literature review, writing of the article; S.N. Bardakov — statistical processing of the results, writing and editing the article; A.M. Emelin — preparation of graphic materials; R.V. Deev — research design, editing the text of the article.

ДОПОЛНИТЕЛЬНАЯ ИНФОРМАЦИЯ

Источник финансирования. Исследование выполнено при финансовой поддержке Министерства науки и высшего образования РФ, соглашение № 075-15-2021-1346.

Конфликт интересов. Авторы декларируют отсутствие явных и потенциальных конфликтов интересов, связанных с публикацией настоящей статьи.

Вклад авторов. Все авторы подтверждают соответствие своего авторства международным критериям ICMJE (все авторы внесли существенный вклад в разработку концепции, проведение исследования и подготовку статьи, прочли и одобрили финальную версию перед публикацией). Наибольший вклад распределён следующим образом: М.А. Савельева — изготовление гистологических препаратов, обзор литературы, подготовка и написание текста статьи; С.Н. Бардаков — статистическая обработка полученных результатов, подготовка и написание текста статьи, редактирование текста; А.М. Емелин — подготовка графических материалов; Р.В. Деев — дизайн исследования, редактирование текста статьи.

REFERENCES

1. Straub V, Murphy A, Udd B; LGMD workshop study group. 229th ENMC international workshop: limb girdle muscular dystrophies — nomenclature and reformed classification Naarden, the Netherlands, 17–19 March 2017. *Neuromuscul Disord*. 2018;28(8):702–710. doi: 10.1016/j.nmd.2018.05.007

2. Mah JK, Korngut L, Fiest KM, et al. A systematic review and meta-analysis on the epidemiology of the muscular dystrophies. *Can J Neurol Sci*. 2016;43(1):163–177. doi: 10.1017/cjn.2015.311

3. Umakhanova ZR, Bardakov SN, Mavlikeev MO, et al. Twenty-year clinical progression of dysferlinopathy in patients from Dagestan. *Front Neurol*. 2017;8:145. doi: 10.3389/fneur.2017.00145

4. Bashir R, Strachan T, Keers S, et al. A gene for autosomal recessive limb-girdle muscular dystrophy maps to chromosome 2p. *Hum Mol Genet.* 1994;3(3):455–457. doi: 10.1093/hmg/3.3.455

5. Folland C, Johnsen R, Botero Gomez A, et al. Identification of a novel heterozygous DYSF variant in a large family with a dominantly-inherited dysferlinopathy. *Neuropathol Appl Neurobiol.* 2022;48(7):e12846. doi: 10.1111/nan.12846

6. Anderson LV, Davison K, Moss JA, et al. Dysferlin is a plasma membrane protein and is expressed early in human development. *Hum Mol Genet.* 1999;8(5):855–861. Corrected and republished from: ***Hum Mol Genet.*** 1999;8(6):1141. doi: 10.1093/hmg/8.5.855

7. Bulankina AV, Thoms S. Functions of vertebrate ferlins. *Cells.* 2020;9(3):534. doi: 10.3390/cells9030534

8. Chernova ON. *Features of structure and reparative histogenesis of transverse striated skeletal muscle tissue in mice with genetically determined dysferlin deficiency* [dissertation]. Saint Petersburg; 2021. EDN: DNCGFD

9. Ho M, Post CM, Donahue LR, et al. Disruption of muscle membrane and phenotype divergence in two novel mouse models of dysferlin deficiency. *Hum Mol Genet*. 2004;13(18):1999–2010. doi: 10.1093/hmg/ddh212

10. Cárdenas AM, González-Jamett AM, Cea LA, et al. Dysferlin function in skeletal muscle: possible pathological mechanisms and therapeutical targets in dysferlinopathies. *Exp Neurol.* 2016;283(Pt A):246–254. doi: 10.1016/j.expneurol.2016.06.026

11. Gayathri N, Alefia R, Nalini A, et al. Dysferlinopathy: spectrum of pathological changes in skeletal muscle tissue. *Indian J Pathol Microbiol*. 2011;54(2):350–354. doi: 10.4103/0377-4929.81636

12. Hofhuis J, Bersch K, Büssenschütt R, et al. Dysferlin mediates membrane tubulation and links T-tubule biogenesis to muscular dystrophy. *J Cell Sci*. 2017;130(5):841–852. doi: 10.1242/jcs.198861

13. Hornsey MA, Laval SH, Barresi R, Lochmüller H, Bushby K. Muscular dystrophy in dysferlin-deficient mouse models. *Neuromuscul Disord*. 2013;23(5):377–387. doi: 10.1016/j.nmd.2013.02.004

14. Chase TH, Cox GA, Burzenski L, et al. Dysferlin deficiency and the development of cardiomyopathy in a mouse model of limb-girdle muscular dystrophy 2B. *Am J Pathol*. 2009;175(6):2299–2308. doi: 10.2353/ajpath.2009.080930

15. Han R, Bansal D, Miyake K, et al. Dysferlin-mediated membrane repair protects the heart from stress-induced left ventricular injury. *J Clin Invest.* 2007;117(7):1805–1813. doi: 10.1172/JCI30848

16. Nishikawa A, Mori-Yoshimura M, Segawa K, et al. Respiratory and cardiac function in japanese patients with dysferlinopathy. *Muscle Nerve.* 2016;53(3):394–401. doi: 10.1002/mus.24741

17. Tan SML, Ong CC, Tan KB, et al. Subclinical cardiomyopathy in Miyoshi myopathy detected by late gadolinium enhancement cardiac magnetic resonance imaging. *Int Heart J*. 2021;62(1):186–192. doi: 10.1536/ihj.20-354

18. Korzhevskiy DE, Gilyarov AV. *Fundamentals of histologic technique*. Saint Petersburg: SpecLit; 2010. 95 p. (In Russ).

19. Mavlikeev MO, Arkhipova SS, Chernova ON, et al. *Short course of histological techniques: educational manual*. Kazan': Kazanskij universitet; 2020. 107 p. (In Russ).

20. Øyvind Hammer DATH, Ryan PD. PAST: Paleontological Statistics Software Package for Education and Data Analysis. ***Palaeontologia Electronica***. 2001;4(1). Available from: https://palaeo-electronica.org/2001_1/past/past.pdf

21. Kraemer HC, Kupfer DJ. Size of treatment effects and their importance to clinical research and practice. *Biol Psychiatry*. 2006;59(11):990–996. doi: 10.1016/j.biopsych.2005.09.014

22. Coe R. *Effect size calculator*. Cambridge CEM; 2000. Available from: https://lbecker.uccs.edu/

23. Wenzel K, Geier C, Qadri F, et al. Dysfunction of dysferlin-deficient hearts. *J Mol Med (Berl)*. 2007;85(11):1203–1214. doi: 10.1007/s00109-007-0253-7

24. Bonda TA, Szynaka B, Sokołowska M, et al. Remodeling of the intercalated disc related to aging in the mouse heart. *J Cardiol.* 2016;68(3):261–268. doi: 10.1016/j.jjcc.2015.10.001
25. Hofhuis J, Bersch K, Wagner S, et al. Dysferlin links excitation-contraction coupling to structure and maintenance of the cardiac transverse-axial tubule system. *Europace.* 2020;22(7):1119–1131. doi: 10.1093/europace/euaa093
26. Maier LS, Bers DM. Calcium, calmodulin, and calcium-calmodulin kinase II: heartbeat to heartbeat and beyond. *J Mol Cell Cardiol.* 2002;34(8):919–939. doi: 10.1006/jmcc.2002.2038
27. Shevchenko YuL, Plotnitsky AV, Sudilovskaya VV, et al. The morphology and markers of the immobilizing interstitial fibrosis of the heart. *Bulletin of Pirogov National Medical & Surgical Center.* 2022;17(3):84–93. EDN: CAKOXR doi: 10.25881/20728255_2022_17_3_84
28. Wei B, Wei H, Jin JP. Dysferlin deficiency blunts β-adrenergic-dependent lusitropic function of mouse heart. *J Physiol.* 2015;593(23):5127–5144. doi: 10.1113/JP271225
29. Suzuki N, Takahashi T, Suzuki Y, et al. An autopsy case of a dysferlinopathy patient with cardiac involvement. *Muscle Nerve.* 2012;45(2):298–299. doi: 10.1002/mus.22247
30. Choi ER, Park SJ, Choe YH, et al. Early detection of cardiac involvement in Miyoshi myopathy: 2D strain echocardiography and late gadolinium enhancement cardiovascular magnetic resonance. Journal of cardiovascular magnetic resonance. *J Cardiovasc Magn Reson.* 2010;12(1):31. doi: 10.1186/1532-429X-12-31

СПИСОК ЛИТЕРАТУРЫ

1. Straub V., Murphy A., Udd B.; LGMD workshop study group. 229th ENMC international workshop: limb girdle muscular dystrophies — nomenclature and reformed classification Naarden, the Netherlands, 17–19 March 2017 // Neuromuscul Disord. 2018. Vol. 28, N 8. P. 702–710. doi: 10.1016/j.nmd.2018.05.007
2. Mah J.K., Korngut L., Fiest K.M., et al. A systematic review and meta-analysis on the epidemiology of the muscular dystrophies // Can J Neurol Sci. 2016. Vol. 43, N 1. P. 163–177. doi: 10.1017/cjn.2015.311
3. Umakhanova Z.R., Bardakov S.N., Mavlikeev M.O., et al. Twenty-year clinical progression of dysferlinopathy in patients from Dagestan // Front Neurol. 2017. Vol. 8. P. 145. doi: 10.3389/fneur.2017.00145
4. Bashir R., Strachan T., Keers S., et al. A gene for autosomal recessive limb-girdle muscular dystrophy maps to chromosome 2p // Hum Mol Genet. 1994. Vol. 3, N 3. P. 455–457. doi: 10.1093/hmg/3.3.455
5. Folland C., Johnsen R., Botero Gomez A., et al. Identification of a novel heterozygous DYSF variant in a large family with a dominantly-inherited dysferlinopathy // Neuropathol Appl Neurobiol. 2022. Vol. 48, N 7. P. e12846. doi: 10.1111/nan.12846
6. Anderson L.V., Davison K., Moss J.A., et al. Dysferlin is a plasma membrane protein and is expressed early in human development // Hum Mol Genet. 1999. Vol. 8, N 5. P. 855–861. Corrected and republished from: Hum Mol Genet 1999. Vol. 8. P. 1141. doi: 10.1093/hmg/8.5.855
7. Bulankina A.V., Thoms S. Functions of vertebrate ferlins // Cells. 2020. Vol. 9, N 3. P. 534. doi: 10.3390/cells9030534
8. Чернова О.Н. Особенности строения и репаративного гистогенеза поперечнополосатой скелетной мышечной ткани у мышей с генетически обусловленным дефицитом дисферлина: дис. … канд. мед. наук. Санкт-Петербург, 2021. EDN: DNCGFD
9. Ho M., Post C.M., Donahue L.R., et al. Disruption of muscle membrane and phenotype divergence in two novel mouse models of dysferlin deficiency // Hum Mol Genet. 2004. Vol. 13, N 18. P. 1999–2010. doi: 10.1093/hmg/ddh212
10. Cárdenas A.M., González-Jamett A.M., Cea L.A., et al. Dysferlin function in skeletal muscle: possible pathological mechanisms and therapeutical targets in dysferlinopathies // Exp Neurol. 2016. Vol. 283(Pt A). P. 246–254. doi: 10.1016/j.expneurol.2016.06.026
11. Gayathri N., Alefia R., Nalini A., et al. Dysferlinopathy: spectrum of pathological changes in skeletal muscle tissue // Indian J Pathol Microbiol. 2011. Vol. 54, N 2. P. 350–354. doi: 10.4103/0377-4929.81636
12. Hofhuis J., Bersch K., Büssenschütt R., et al. Dysferlin mediates membrane tubulation and links T-tubule biogenesis to
muscular dystrophy // J Cell Sci. 2017. Vol. 130, N 5. P. 841–852. doi: 10.1242/jcs.198861
13. Hornsey M.A., Laval S.H., Barresi R., et al. Muscular dystrophy in dysferlin-deficient mouse models // Neuromuscul Disord. 2013. Vol. 23, N 5. P. 377–387. doi: 10.1016/j.nmd.2013.02.004
14. Chase T.H., Cox G.A., Burzenski L., et al. Dysferlin deficiency and the development of cardiomyopathy in a mouse model of limb-girdle muscular dystrophy 2B // Am J Pathol. 2009. Vol. 175, N 6. P. 2299–2308. doi: 10.2353/ajpath.2009.080930
15. Han R., Bansal D., Miyake K., et al. Dysferlin-mediated membrane repair protects the heart from stress-induced left ventricular injury // J Clin Invest. 2007. Vol. 117, N 7. P. 1805–1813. doi: 10.1172/JCI30848
16. Nishikawa A., Mori-Yoshimura M., Segawa K., et al. Respiratory and cardiac function in japanese patients with // Muscle Nerve. 2016. Vol. 53, N 3. P. 394–401. doi: 10.1002/mus.24741
17. Tan S.M.L., Ong C.C., Tan K.B., et al. Subclinical cardiomyopathy in miyoshi myopathy detected by late gadolinium enhancement cardiac magnetic resonance imaging // Int Heart J. 2021. Vol. 62, N 1. P. 186–192. doi: 10.1536/ihj.20-354
18. Коржевский Д.Э., Гиляров А.В. Основы гистологической техники. Санкт-Петербург: СпецЛит, 2010. 95 с. EDN: RTTUSB
19. Мавликеев М.О., Архипова С.С., Чернова О.Н., и др. Краткий курс гистологической техники: учебно-методическое пособие. Казань: Казанский университет, 2020. 107 с.
20. Øyvind Hammer D.A.T.H., Ryan P.D. PAST: Paleontological Statistics Software Package for Education and Data Analysis // Palaeontologia Electronica. 2001. Vol. 4, N 1. Режим доступа: https://palaeo-electronica.org/2001_1/past/past.pdf
21. Kraemer H.C., Kupfer D.J. Size of treatment effects and their importance to clinical research and practice // Biol Psychiatry. 2006. Vol. 59, N 11. P. 990–996. doi: 10.1016/j.biopsych.2005.09.014
22. Coe R. Effect size calculator. Cambridge CEM, 2000. Режим доступа: https://lbecker.uccs.edu/
23. Wenzel K., Geier C., Qadri F., et al. Dysfunction of dysferlin-deficient hearts // J Mol Med (Berl). 2007. Vol. 85, N 11. P. 1203–1214. doi: 10.1007/s00109-007-0253-7
24. Bonda T.A., Szynaka B., Sokołowska M., et al. Remodeling of the intercalated disc related to aging in the mouse heart // J Cardiol. 2016. Vol. 68, N 3. P. 261–268. doi: 10.1016/j.jjcc.2015.10.001
25. Hofhuis J., Bersch K., Wagner S., et al. Dysferlin links excitation-contraction coupling to structure and maintenance of the cardiac

transverse-axial tubule system // Europace. 2020. Vol. 22, N 7. P. 1119–1131. doi: 10.1093/europace/euaa093
26. Maier L.S., Bers D.M. Calcium, calmodulin, and calcium-calmodulin kinase II: heartbeat to heartbeat and beyond // J Mol Cell Cardiol. 2002. Vol. 34, N 8. P. 919–939. doi: 10.1006/jmcc.2002.2038
27. Шевченко Ю.Л., Плотницкий А.В., Судиловская В.В., и др. Морфология маркеры иммобилизирующего интерстициального фиброза сердца // Вестник Национального медико-хирургического Центра им. Н.И. Пирогова. 2022. Т. 17, № 3. 84–93. EDN: CAKOXR doi: 10.25881/20728255_2022_17_3_84
28. Wei B., Wei H., Jin J.P. Dysferlin deficiency blunts β-adrenergic-dependent lusitropic function of mouse heart // J Physiol. 2015. Vol. 593, N 23. P. 5127–5144. doi: 10.1113/JP271225
29. Suzuki N., Takahashi T., Suzuki Y., et al. An autopsy case of a dysferlinopathy patient with cardiac involvement // Muscle Nerve. 2012. Vol. 45, N 2. P. 298–299. doi: 10.1002/mus.22247
30. Choi E.R., Park S.J., Choe Y.H., et al. Early detection of cardiac involvement in Miyoshi myopathy: 2D strain echocardiography and late gadolinium enhancement cardiovascular magnetic resonance // J Cardiovasc Magn Reson. 2010. Vol. 12, N 1. P. 31. doi: 10.1186/1532-429X-12-31

AUTHORS' INFO

*** Maria A. Savelyeva;**
address: 47 Piskarevskij avenue, 195067 Saint Petersburg, Russia;
ORCID: 0009-0008-5667-115X;
eLibrary SPIN: 9935-5416;
e-mail: savelyeva.mariaanat@yandex.ru

Sergey N. Bardakov, MD, Cand. Sci. (Medicine);
ORCID: 0000-0002-3804-6245;
eLibrary SPIN: 2351-4096;
e-mail: epistaxis@mail.ru

Alexey M. Emelin;
ORCID: 0000-0003-4109-0105;
eLibrary SPIN: 5605-1140;
e-mail: eamar40rn@gmail.com

Roman V. Deev, MD, Cand. Sci. (Medicine), Assistant Professor;
ORCID: 0000-0001-8389-3841;
eLibrary SPIN: 2957-1687;
e-mail: romdey@gmail.com

* Corresponding author / Автор, ответственный за переписку

ОБ АВТОРАХ

*** Савельева Мария Анатольевна;**
адрес: Россия, 195067, Санкт-Петербург, Пискаревский пр-т, д. 47;
ORCID: 0009-0008-5667-115X;
eLibrary SPIN: 9935-5416;
e-mail: savelyeva.mariaanat@yandex.ru

Бардаков Сергей Николаевич, канд. мед. наук;
ORCID: 0000-0002-3804-6245;
eLibrary SPIN: 2351-4096;
e-mail: epistaxis@mail.ru

Емелин Алексей Михайлович;
ORCID: 0000-0003-4109-0105;
eLibrary SPIN: 5605-1140;
e-mail: eamar40rn@gmail.com

Деев Роман Вадимович, канд. мед. наук, доцент;
ORCID: 0000-0001-8389-3841;
eLibrary SPIN: 2957-1687;
e-mail: romdey@gmail.com